Eur. Phys. J. D **28**, 187–192 (2004)
DOI: 10.1140/epjd/e2003-00307-2

THE EUROPEAN PHYSICAL JOURNAL D

Close-coupling calculations of spectral line shape parameters for Cd($5^3P_1 - 5^1S_0$) in a bath of noble gases

T. Orlikowski[a]

Institute of Physics, Nicolaus Copernicus University, 87-100 Toruń, Poland

Received 20 January 2003 / Received in final form 10 July 2003
Published online 9 December 2003 –

Abstract. Line shape parameters of the intercombination line $5^3P_1 - 5^1S_0$ of cadmium ($\lambda = 326.1$ nm) perturbed by noble gas atoms are calculated by the quantum close-coupling method. Calculations are based on the ab initio potential curves determined by Czuchaj and Stoll. The obtained values of width and shift coefficients are compared with experimental data and some other theoretical results.

PACS. 32.70.-n Intensities and shapes of atomic spectral lines – 34.50.-s Scattering of atoms and molecules

1 Introduction

The most widely applied theory of pressure broadening of spectral lines is the semiclassical impact approach introduced by Anderson [1] with further extensions and improvements (for details see the comprehensive reviews by Allard and Kielkopf [2] and by Peach [3]). The collision trajectories are described classically and the semiclassical equations that determine the S-matrix are solved. The fully quantum theory which relates pressure broadening to the emitter–perturber interaction potential via quantum-mechanical treatment of collision dynamics is also well developed [4–7]. Since the pioneering work of Shafer and Gordon [6] on the rotational Raman spectrum of H_2 perturbed by He, the rigorous theory has been used quite successfully to predict the line width and shift of a few atomic [8–11] as well as molecular [12–15] systems. Motivated by the recent experimental investigations by Bielski's group [16–24] we have undertaken a companion fully quantum mechanical close-coupling studies on the $5^3P_1 - 5^1S_0$ intercombination line of ^{114}Cd perturbed by noble gas atoms.

2 Spectral line shape expressions

The quantum formalism for collisional broadening of spectral lines in which both the emitter and perturber are treated quantum mechanically has been discussed by many authors both for ro-vibrational molecular spectra as well as for atomic ones. Only the relevant features of the theory will be summarized here.

The spectral line shape function $I(\omega)$ is usually defined as the Fourier transform of the autocorrelation function of the coupling operator between radiating system and the external electromagnetic field. According to the general relaxation theory of gas mixtures developed by Fano [25] and elaborated in details for the pressure broadening and shift of spectral lines by Ben-Reuven [26] the line shape function is given by

$$I(\omega) = -\pi^{-1}\mathrm{Im}\,\mathrm{Tr}_s\left\{A\left(\omega - L_o^s - \Lambda\right)^{-1}\rho_s A\right\}, \qquad (1)$$

where L_o^s is the Liouville operator for the unperturbed active system, ρ_s is the corresponding density operator, A is the coupling operator between the system and the external field, and Λ is the relaxation operator which describe the influence of the bath on the system of interest. Subscripts s and b refer to the system and bath variables, respectively. In general, Λ is a complicated operator with respect to the system variables and depends on radiation frequency, ω, and the density of the perturber gas, n_b. Under the commonly applied impact approximation and including the effects of only binary collisions Λ is independent of ω and depends linearly on n_b, and is given by [25]

$$\Lambda = n_b\,\mathrm{Tr}_b\left\{\rho_b m\right\}. \qquad (2)$$

where m is the binary collision operator defined as

$$m = T_\alpha - T_\beta^+ + 2\pi i\, T_\alpha T_\beta^+. \qquad (3)$$

Here T_α and T_β are the transition operators, which describe scattering in the initial and final spectroscopic states, respectively. The T operators are evaluated at the same kinetic energy. The trace in equation (1) can be conveniently evaluated in terms of a basis of eigenstates of the unperturbed emitter. Applying this basis we can write

[a] e-mail: torl@phys.uni.torun.pl

explicitly the line shape function in the form

$$I(\omega) = -\pi^{-1}\mathrm{Im}\sum_{\alpha,\alpha',\beta,\beta'} A^*_{\alpha'\beta'}[\omega - \omega_{\alpha\beta} - in_b\langle v\sigma_s(\alpha'\beta',\alpha\beta)\rangle]^{-1}\rho_\alpha A_{\alpha\beta}, \quad (4)$$

where $A_{\alpha\beta}$ is the reduced matrix element of the operator A, v is the relative velocity before collision, ρ_α is the Boltzmann distribution factor for the emitter level populations, and the acute brackets denote the thermal averaging over the relative kinetic energy. In equation (4) we have expressed the operator m by the phenomenological line broadening cross-section, σ_s. The initial and final spectroscopic states after collision are indicated by primes.

Expression (4) gives the shape of an entire band. At low pressure when individual lines are well resolved only the diagonal cross-sections are important and in such a case the shape of a spectral band appears as a sum of Lorentzian lines, for which the line width is given by the real part of the cross-section

$$\Gamma_{\alpha\beta} = n_b\mathrm{Re}\langle v\sigma_s(\alpha\beta,\alpha\beta)\rangle \quad (5)$$

and the line shift is given by the imaginary part

$$\Delta_{\alpha\beta} = -n_b\mathrm{Im}\langle v\sigma_s(\alpha\beta,\alpha\beta)\rangle. \quad (6)$$

The off-diagonal elements of σ_s describe the interference of overlapping lines and result in deviation from the Lorentzian shape.

Equations (4–6) are the fundamental relationships between the collision dynamics and the spectral line profiles. The required S or T matrices which contain the relevant scattering information could be determined by the exact quantum close-coupling method as well as by approximate scattering methods quantum or semiclassical.

In this paper we consider the intermultiplet transitions involving initial and final emitter levels characterized by j_i and j_f, respectively. The respective expression for the pressure broadening cross-section is of the form [6,7]

$$\sigma_s(j_ij_f, j_i'j_f') = \frac{\pi}{k_j^2}\sum_{ll'J_iJ_f}(2J_i+1)(2J_f+1)(-1)^{l+l'}\begin{Bmatrix} j_i' & q & j_f' \\ J_f & l' & J_i\end{Bmatrix}\begin{Bmatrix} j_i & q & j_f \\ J_f & l & J_i\end{Bmatrix} \times\left[\delta_{ll'}\delta_{j_ij_i'}\delta_{j_fj_f'} - S^{J_i}(j_i'l', j_il)S^{*J_f}(j_f'l', j_fl)\right]. \quad (7)$$

Here l and J are the quantum numbers for the orbital and total angular momenta, respectively; q is the tensor rank of spectral transition (for dipole spectra $q = 1$). Subscripts i and f label the initial and final spectral levels; unprimed and primed quantities refer to values before and after a collision, respectively.

3 Scattering equations

The quantum formalism for inelastic collision of an atom with structureless particle has been provided by Mies [27] and Alexander and co-workers [28]. Only the relevant details will be reviewed here.

The total Hamiltonian of the diatomic system considered here is

$$H(\mathbf{R},\mathbf{r}) = -\frac{\hbar^2}{2\mu R^2}\frac{d}{dR}\left(R^2\frac{d}{dR}\right) + H_{rot}(\widehat{\mathbf{R}}) + V_{LS}(\mathbf{R},\mathbf{r}) + H^o_{EP}(\mathbf{R},\mathbf{r}), \quad (8)$$

where μ is the reduced mass, R is the interatomic distance, $\mathbf{r}$ represents the set of electronic coordinates, H_{rot} is the Hamiltonian for the orbital motion of the two nuclei, the last term represents the electronic Hamiltonian of the isolated emitter and perturber atoms and their mutual electrostatic interaction:

$$H^o_{EP}(\mathbf{R},\mathbf{r}) = H_E(\mathbf{r}) + H_P(\mathbf{r}) + V(\mathbf{R},\mathbf{r}). \quad (9)$$

The fine-structure term, V_{LS}, has been separated to facilitate discussion of the interaction matrix elements.

Following the standard close-coupling (CC) method of Arthurs and Dalgarno [29] the total scattering wave function is expanded in terms of the channel states that are eigenfunctions of the total angular momentum of the collision system, namely

$$\psi^{JM}(\mathbf{r},\mathbf{R}) = R^{-1}\sum_{jl}F^{JM}_{jl}(R)|R;jlJM\rangle, \quad (10)$$

where the channel states $|R;jlJM\rangle$ are constructed according to the Hund's case (e) coupling scheme and are given by [27,28]

$$|R;jlJM\rangle = \sum_{\Lambda\Sigma\Omega}(-1)^{j+\Omega}C(Jjl;-\Omega\Omega0) \times C(LSj;\Lambda\Sigma\Omega)|JM\Omega\rangle|R,\Lambda\Sigma\rangle, \quad (11)$$

where $C(...;...)$ are the Clebsch-Gordan coefficients, $|JM\Omega\rangle$ are the normalized symmetric-top wave functions:

$$|JM\Omega\rangle = \left(\frac{2J+1}{4\pi}\right)^{1/2}D^{J^*}_{M\Omega}(\phi,\theta,0), \quad (12)$$

and $|R,\Lambda\Sigma\rangle$ designate the electronic states of the emitter-perturber pair which define the corresponding adiabatic potentials

$$H^o_{EP}|R,\Lambda\Sigma\rangle = {}^{2S+1}W_\Lambda(R)|R,\Lambda\Sigma\rangle. \quad (13)$$

Asymptotically, when $V \to 0$, the total electronic Hamiltonian becomes diagonal with good quantum numbers L, S, j, l, J, M, which denote, respectively, the electronic, spin and total angular momentum of the emitter, the emitter-perturber orbital angular momentum, and finally, the total angular momentum and its projection along a space-fixed axis. The projections of L, S and J along the emitter-perturber axis are traditionally designated by Λ, Σ and Ω, respectively.

Following the previous treatments [8,28] on collisions involving atoms in multiplet electronic states we assume

that L remains a good quantum number at all values of R. In this so-called "pure precession" limit [30] the rotational and spin-orbit Hamiltonians are diagonal in the basis (11) with matrix elements given by

$$\langle jlJM|H_{rot}+V_{LS}|j'l'JM\rangle = \delta_{jj'}\delta_{ll'}\left[\frac{\hbar^2}{2\mu R^2}l(l+1)+\varepsilon_j(R)\right], \quad (14)$$

where in our calculations the energies $\varepsilon_j(R)$ have been replaced by their asymptotic values $\varepsilon_j(\infty)$, i.e. the corresponding fine-structure energy levels of the emitter atom. The energy values used for the fine structure splitting are those reported by Moore [31], i.e. $\varepsilon(5\,^3\mathrm{P}_1)-\varepsilon(5\,^3\mathrm{P}_0) = 542.113\ \mathrm{cm}^{-1}$ and $\varepsilon(5\,^3\mathrm{P}_1)-\varepsilon(5\,^3\mathrm{P}_2) = -1170.866\ \mathrm{cm}^{-1}$.

Since L is not a good quantum number at small R the pure precession approximation will become, in general, increasingly less accurate as R decreases. To get some insight into mechanism and validity of this approximation we performed a test calculations replacing the rotational term $l(l+1)/R^2$ by $J(J+1)/R^2$ for all channels. The changes in the broadening cross-sections (7) were in the range of 0.2% for Cd–He to 0.1% for Cd–Xe. Similar observation has been made previously for He–He collisions [8]. One might therefore expect that at least for collisions involving closed shell partner the pure precession approximation is in a great measure justified.

Within the commonly applied Born-Oppenheimer approximation the R-dependent expansion coefficients $F(R)$ are solutions to a set of coupled equations [29]

$$\left[\frac{d^2}{dR^2}+k_j^2-\frac{l(l+1)}{R^2}\right]F^J_{jl}(R)=\frac{2\mu}{\hbar^2}\sum_{j'l'}V^J_{jlj'l'}(R)F^J_{j'l'}(R), \quad (15)$$

where k_j is the wavenumber in the (jl) channel defined as

$$k_j^2=\frac{2\mu}{\hbar^2}[E-\varepsilon_j(\infty)], \quad (16)$$

and the coupling matrix elements are [8,27,28]

$$V^J_{jlj'l'}(R)=\sum_{\Omega}(-1)^{j'-j}C(Jjl;-\Omega\Omega0)C(Jj'l';-\Omega\Omega0) \times\sum_{\Lambda\Sigma}C(LSj;\Lambda\Sigma\Omega)C(LSj';\Lambda\Sigma\Omega)\,{}^{2S+1}W_\Lambda(R). \quad (17)$$

From the asymptotic behavior of the solutions to the CC equations (15) one can extract the S-matrix elements in the total J representation [29]. To calculate the broadening cross-sections from expression (7) one requires the S-matrices for lower and upper states evaluated at the same value of relative kinetic energy. The computed S-matrices can also be exploited to calculate the degeneracy averaged cross-section for the $j\to j'$ intramultiplet transition from the expression [29]

$$\sigma_{j\to j'}=\frac{\pi}{k_j^2(2j+1)}\sum_{Jll'}(2J+1)|\delta_{ll'}-S^J_{jlj'l'}|^2. \quad (18)$$

4 Computational details and results for the Cd($5^3\mathrm{P}_1-5^1\mathrm{S}_0$) line

For the considered line the CC equations are required only for ^{1}S and ^{3}P multiplets. The explicitly evaluated potential matrix elements (16) are given by [8,28]:

For the $^1\mathrm{S}_0$ level $L=0$, $S=0$, $j=0$ so that $\Lambda=0$ and

$$V_{jlj'l'}(R)=\delta_{jj'}\delta_{ll'}\,{}^1W_\Sigma(R). \quad (19)$$

For the $^3\mathrm{P}_j$ levels $L=1$, $S=1$ and $j=0$, 1, 2 so that $|\Lambda|=0,1$ and

$$V_{jlj'l'}(R)=\delta_{jj'}\delta_{ll'}\,{}^1W_\Pi(R) + C_{jlj'l'}\left[{}^3W_\Sigma(R)-{}^3W_\Pi(R)\right], \quad (20)$$

where

$$C_{jlj'l'}=\sum_{\Omega}(-1)^{j'-j}C(Jjl;-\Omega\Omega0)C(Jj'l';0\Omega\Omega) \times C(11j;0\Omega\Omega)C(11j';0\Omega\Omega). \quad (21)$$

In equations (19, 20) $^1W_\Sigma$, $^3W_\Sigma$ and $^3W_\Pi$ are the adiabatic electrostatic potential curves of Σ and Π symmetry which arise from interaction of Cd atom in the ground and excited states with neutral perturber.

The present calculations are based on potential curves determined by Czuchaj and Stoll [32] within a pseudopotential self-consistent field/configuration interaction (SCF/CI) method. In this approach only the valence electrons of the interacting atoms have been explicitly treated by quantum-chemical calculations while the atomic cores were modelled by the l-dependent pseudopotentials. The fairly good agreement of the theoretical and experimental values of spectroscopic parameters (D_e, R_e, ω_e) indicates that the calculated potential curves represent globally reliable description of the Cd – noble gas interaction at least for short and intermediate interatomic distances. However, the quality of the theoretical potentials can only be judged by comparison with experimental data. One of the purposes of the present work is to investigate how well these potentials reproduce the experimental line width and shift parameters using accurate quantum-mechanical treatment of the collision dynamics. These potentials were computed at over 40 internuclear distances in the range $3<R<30a_0$ what cover the relevant region for scattering calculations. Explicit representations of these potentials required in numerical calculations were obtained by the cubic spline fitting between the ab initio points.

In the present work the CC equations were solved by using the log-derivative method of Johnson [35] with an integration step equal to $0.01a_0$. The integration have been performed from $R=3a_0$ up to some R_{max} value at which convergent S-matrix elements were extracted. The real and imaginary parts of the pressure broadening cross-section defined by equation (7) were calculated for the relative kinetic energy in the range $0<E\le0.06$ au, wide enough to perform the energy averaging for higher

Table 1. Pressure width coefficients (in units of 10^{-20} cm^{-1}/atom cm^{-3}) for the 326.1 nm Cd line perturbed by noble gases at 468 and 724 K. For experimental data the values of standard uncertainty are given.

	$T = 468$ K				$T = 724$ K			
Perturber	β_{cc}	$\beta_{\overline{v}}$	β_{exp}	β_{sc}	β_{cc}	$\beta_{\overline{v}}$	β_{exp}	β_{sc}
He	1.114	1.055	1.22 ± 0.03^a	1.40^a	1.283	1.261	–	–
Ne	0.722	0.764	0.70 ± 0.02^a	0.84^a	0.806	0.857	0.715 ± 0.004^e	0.750^e
Ar	1.293	1.428	1.04 ± 0.02^b	1.74^b	1.453	1.618	1.060 ± 0.006^f	1.334^f
Kr	1.157	1.212	1.00 ± 0.03^c	1.47^c	1.371	1.299	1.147 ± 0.011^g	1.182^g
Xe	1.263	1.297	1.32 ± 0.03^d	1.85^d	1.466	1.487	1.257 ± 0.006^h	1.330^h

[a] Refs. [20,21], [b] Ref. [22], [c] Ref. [23], [d] Ref. [24], [e] Ref. [16], [f] Ref. [17], [g] Ref. [18], [h] Ref. [19].

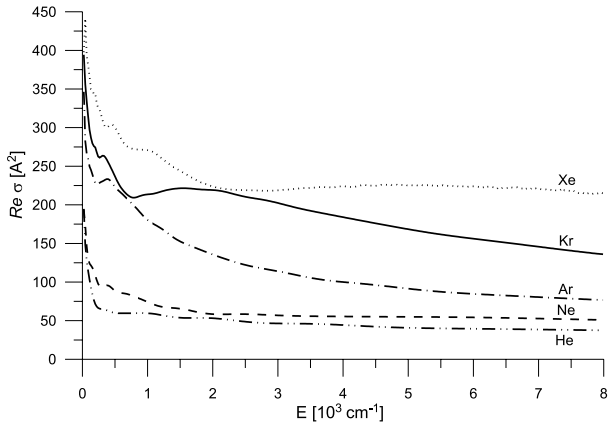

Fig. 1. Width cross-sections plotted as a function of kinetic energy for the Cd 326.1 nm line perturbed by noble gases.

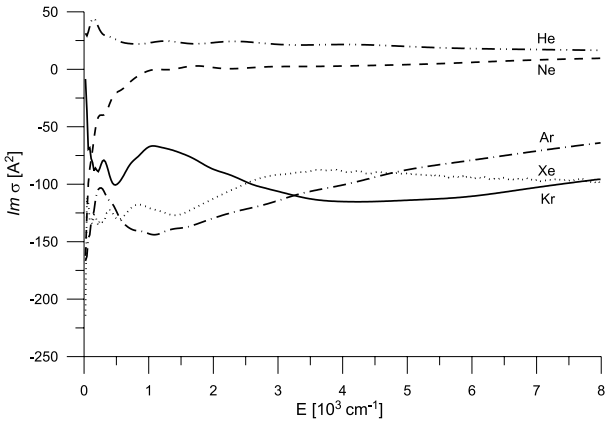

Fig. 2. Shift cross-sections plotted as a function of kinetic energy for the Cd 326.1 nm line perturbed by noble gases.

temperatures ($T > 400$ K). For energies below the excitation threshold $\epsilon(5\,^3P_2)$ the closed channels associated with $j = 2$ were retained in our calculations. The resulted width and shift cross-sections for noble gas perturbers from He to Xe are plotted as a function of kinetic energy in Figures 1 and 2, respectively.

The width cross-sections for all perturbers exhibit a common feature, they decrease rapidly with energy and then for $E > 0.01$ au monotonically approach their limiting values. The shift cross-sections displayed in Figure 2 show slightly more complex structure. At low energies they are negative except of the cross-section for helium which is positive for all considered energies. For the case of neon the shift cross-section change sign in the vicinity of 0.005 au and then attains positive asymptotic value. Furthermore, we observe in Figure 2 that the shift cross-sections at sufficiently high energies also approach their asymptotic values.

Since both the line width and shift at low pressure depend linearly on the density of perturbing atoms and for isolated line σ_s reduces to a single complex number it is convenient to rewrite equations (5, 6) in the abbreviated form: $\Gamma = n_b\beta$ and $\Delta = n_b\delta$, where β and δ are the pressure width and shift coefficients, respectively. Scattering calculations were done at a variety of translational energies in order to perform thermal averaging over Maxwellian distribution. The accurate integration over perturber velocities was performed using Simpson's methods.

Averages of the β and δ coefficients were calculated at temperatures of 468 and 724 K, which exactly correspond to the interferometric [20–24] and laser induced fluorescence [16–19] line broadening experiments by Bielski and co-workers. The corresponding set of obtained results is presented in Tables 1 and 2, together with experimental and some other theoretical data. Calculations employing semiclassical (SC) procedures have been performed previously for all these systems [16–24] exploiting the ab initio potentials supplied by Czuchaj and co-workers [32–34] as well as some model potential curves. In Tables 1 and 2 we have quoted only the SC results obtained for the ab initio potentials. The SC calculations are based on the Baranger's impact theory with the use of semiclassical description of scattering. Straight-line perturber trajectories were used to calculate the β and δ coefficients.

A comparison of CC and SC line width coefficients in Table 1 for 468 K shows that the CC results are significantly smaller and generally agree better with experimental data for all perturbers. However, the direct comparison is obscured by the use of slightly different version of Czuchaj's potential curves in the SC calculations. For the temperature of 724 K the calculated width coefficients reveal on average about 15% growth, which is not seen in the experimental data except of the value for Kr which is about 15% larger. Also no clear temperature dependence of the width coefficients was seen in the experimental data for He and Ar reported by Dietz et al. [36]. In order to understand this temperature behavior the line

Table 2. Pressure shift coefficients (in units of 10^{-20} cm^{-1}/atom cm^{-3}) for the 326.1 nm Cd line perturbed by noble gases at 468 and 724 K. For experimental data the values of standard uncertainty are given.

	$T = 468$ K				$T = 724$ K			
Perturber	δ_{cc}	$\delta_{\overline{v}}$	δ_{exp}	δ_{sc}	δ_{cc}	$\delta_{\overline{v}}$	δ_{exp}	δ_{sc}
He	0.234	0.237	0.02 ± 0.02^a	0.15^a	0.269	0.241	–	–
Ne	–0.099	–0.111	-0.13 ± 0.01^a	0.08^a	–0.071	–0.075	-0.090 ± 0.005^e	-0.142^e
Ar	–0.392	–0.355	-0.29 ± 0.03^b	-0.58^b	–0.499	–0.518	-0.387 ± 0.004^f	-0.358^f
Kr	–0.199	–0.230	-0.27 ± 0.03^c	-0.77^c	–0.245	–0.268	-0.338 ± 0.005^g	-0.181^g
Xe	–0.269	–0.263	-0.31 ± 0.02^d	-0.83^d	–0.325	–0.336	-0.348 ± 0.002^h	-0.322^h

[a] Refs. [20,21], [b] Ref. [22], [c] Ref. [23], [d] Ref. [24], [e] Ref. [16], [f] Ref. [17], [g] Ref. [18], [h] Ref. [19].

Table 3. De-excitation rates (in units of cm^3 s^{-1}) for the $j \to j'$ fine-structure transitions in collisions of Cd with noble gases. Numbers in parentheses represent powers of 10.

	$T = 468$ K			$T = 724$ K		
Perturber	$1 \to 0$	$2 \to 0$	$2 \to 1$	$1 \to 0$	$2 \to 0$	$2 \to 1$
He	0.466(–16)	0.201(–16)	0.168(–15)	0.459(–15)	0.303(–16)	0.846(–15)
Ne	0.112(–18)	0.570(–17)	0.456(–16)	0.636(–18)	0.833(–17)	0.519(–16)
Ar	0.696(–20)	0.265(–18)	0.508(–17)	0.102(–18)	0.783(–18)	0.779(–17)
Kr	0.129(–20)	0.563(–19)	0.285(–17)	0.468(–20)	0.290(–18)	0.823(–17)
Xe	0.109(–18)	0.150(–16)	0.211(–14)	0.180(–18)	0.109(–15)	0.745(–14)

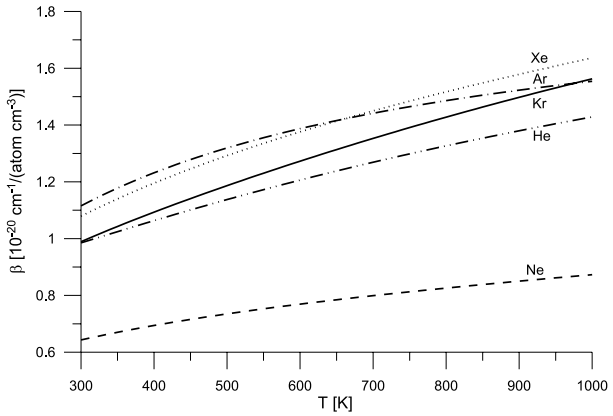

Fig. 3. Temperature dependence of the width coefficients for the Cd 326.1 nm line perturbed by noble gases.

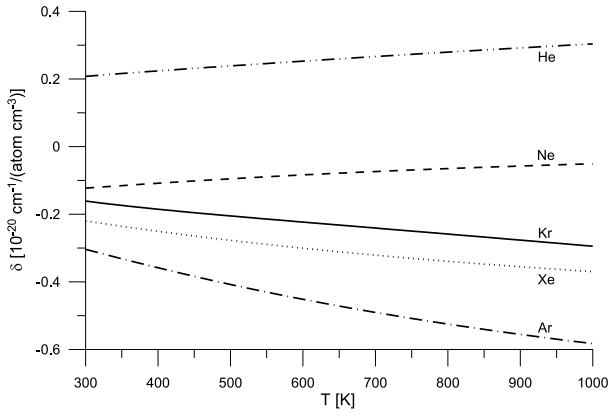

Fig. 4. Temperature dependence of the shift coefficients for the Cd 326.1 nm line perturbed by noble gases.

shape coefficients were calculated for a grid of temperatures over the range 300−1000 K. Figures 3 and 4 illustrate the temperature dependence of the β and δ coefficients, respectively. We observe in Figure 3 that the width coefficients for all perturbers rise very slowly with increasing temperature. Within the considered range of temperature the growth is nearly linear for He, Ne and Kr.

For the case of line shift the results in Table 2 show again that for 468 K the CC coefficients are in better agreement with experimental data than the SC ones except of shifts for helium. The poor agreement for helium is also seen for semiclassical results. Inspection of the shifts for 724 K shows that generally the CC results are in slightly worse agreement with experimental data than the SC values. The calculated temperature behavior of the shift coefficients displayed in Figure 4 indicates for linear and rather weak dependence on temperature for all considered perturbers.

In order to assess the influence of the proper thermal averaging on the theoretically predicted line shape coefficients we performed additional calculations in which the averages over the Maxwellian distribution were replaced by fixed mean velocity, which corresponds to the temperature T, under consideration. The respective coefficients β and δ are labeled by superscript $\overline{v}$ in Tables 1 and 2. The most immediate observation is that the CC coefficients using the $\overline{v}$ approximation are in fairly good qualitative agreement with those explicitly thermally averaged. For the considered Cd line the error does not exceed 10% for all perturbers.

The $5^3\mathrm{P}_j$ triplet S-matrix elements were also used to calculate the fine-structure-changing cross-sections from equation (18). The cross-sections were subsequently averaged over Maxwellian distribution of relative velocity and the corresponding thermal rates, $k_{j\to j'} = \langle v\sigma_{j\to j'}\rangle$, were obtained. De-excitation rates for the three independent intramultiplet transitions for the two considered temperatures are presented in Table 3. We found that the rate coefficients are rather small ($< 10^{-14}$ cm^3 s^{-1}), which is consistent with previous experimental data for collisions of

Cd with CH_4 [37] and He [38]. We also found that among the three transitions the $j = 2 \rightarrow 1$ is the strongest for all considered cases. A more careful analysis of the data in Table 3 shows that: $k_{2\rightarrow1} > k_{2\rightarrow0} > k_{1\rightarrow0}$, except for helium where the $1 \rightarrow 0$ transition is favored over the $2 \rightarrow 0$ transition. The small cross-sections for intramultiplet relaxation of $Ca(5^3P_j)$ indicate that an influence of inelastic collisions on the investigated collisional broadening is negligible for this system.

Our theoretical results are generally in satisfactory agreement with the experimental data. The existing discrepancies could arise both from the choice of interaction potentials and from simplifications in the collision dynamics. In our opinion the applied potentials are primarily responsible for this differences between theory and experiment.

The work reported here was supported by Polish Committee for Scientific Research (KBN) Grant No. 5 P03B 066 20.

References

1. P.W. Anderson, Phys. Rev. **76**, 647 (1949)
2. N. Allard, J. Kielkopf, Rev. Mod. Phys. **54**, 1103 (1982)
3. G. Peach, *Atomic, Molecular and Optical Physics Handbook*, edited by G.W.F. Drake (American Institute of Physics Press, Woodbury, New York, 1996), Chap. 57
4. M. Baranger, Phys. Rev. **111**, 481 (1958); **111**, 494 (1958); **112**, 855 (1958)
5. A.C. Kolb, H. Griem, Phys. Rev. **111**, 514 (1958)
6. R. Shafer, R.G. Gordon, J. Chem. Phys. **58**, 5422 (1973)
7. G. Peach, Comment. At. Mol. Phys. **11**, 101 (1982); K.S. Barnes, G. Peach, J. Phys. B: At. Mol. Phys. **3**, 350 (1970)
8. P.J. Leo, G. Peach, I.B. Whittingham, J. Phys. B: At. Mol. Opt. Phys. **28**, 591 (1995)
9. P.J. Leo, D.F.T. Mullamphy, G. Peach, I.B. Whittingham, J. Phys. B: At. Mol. Opt. Phys. **28**, 4449 (1995); P.J. Leo, D.F.T. Mullamphy, G. Peach, V. Venturi, I.B. Whittingham, J. Phys. B: At. Mol. Opt. Phys. **29**, 4573 (1996); **30**, 535 (1997)
10. A.D. Wilson, Y. Shimoni, J. Phys. B: At. Mol. Phys. **8**, 2415 (1975)
11. T.S. Monteiro, I.L. Cooper, A.S. Dickinson, E.L. Lewis, J. Phys. B: At. Mol. Opt. Phys. **19**, 4087 (1986); **20**, 741 (1987)
12. S. Green, J. Boissoles, C. Boulet, J. Quant. Spectrosc. Radiat. Transfer **39**, 33 (1988)
13. S. Green, J. Chem. Phys. **92**, 4679 (1990); **95**, 3888 (1991); **93**, 1496 (1990); S. Green, J. Hutson, J. Chem. Phys. **100**, 891 (1994)
14. C. Luo, R. Wehr, J.R. Drummond, A.D. May, F. Thibault, J. Boissoles, M. Launay, C. Boulet, J.P. Bounich, J.M. Hartmann, J. Chem. Phys. **115**, 2198 (2001)
15. C.F. Roche, J.M. Hutson, A.S. Dickinson, J. Quant. Spectrosc. Radiat. Transf. **53**, 153 (1995); C.F. Roche, A. Ernesti, J.M. Hutson, A.S. Dickinson, J. Chem. Phys. **104**, 2156 (1996); C.F. Roche, A.S. Dickinson, A. Ernesti, J.M. Hutson, J. Chem. Phys. **107**, 1824 (1997)
16. A. Bielski, D. Lisak, R.S. Trawiński, J. Szudy, Acta Phys. Pol. A. **103**, 23 (2003)
17. A. Bielski, D. Lisak, R.S. Trawiński, Eur. Phys. J. D **14**, 27 (2001)
18. R.S. Trawiński, A. Bielski, D. Lisak, Acta Phys. Pol. A **99**, 243 (2001)
19. A. Bielski, R. Ciuryło, J. Domysławska, D. Lisak, R.S. Trawiński, J. Szudy, Phys. Rev. A **62**, 032511 (2000)
20. A. Bielski, S. Brym, R. Ciuryło, J. Domysławska, E. Lisicki, R.S. Trawiński, J. Phys. B: At. Mol. Opt. Phys. **27**, 5863 (1994)
21. A. Bielski, S. Brym, R. Ciuryło, J. Domysławska, M.G. Lednev, R.S. Trawiński, Acta Phys. Pol. A **90**, 1155 (1996)
22. S. Brym, R. Ciuryło, E. Lisicki, R.S. Trawiński, Phys. Scripta **56**, 541 (1996)
23. S. Brym, J. Domysławska, Phys. Scripta **52**, 511 (1995)
24. S. Brym, R. Ciuryło, R.S. Trawiński, A. Bielski, Phys. Rev. A **56**, 4501 (1997)
25. U. Fano, Phys. Rev. **131**, 259 (1963)
26. A. Ben-Reuven, Phys. Rev. **145**, 7 (1966)
27. F.H. Mies, Phys. Rev. A **7**, 942 (1973)
28. M.H. Alexander, T. Orlikowski, J.E. Straub, Phys. Rev. A **28**, 73 (1983); T. Orlikowski, M.H. Alexander, J. Phys. B: At. Mol. Phys. **17**, 2269 (1984)
29. A.M. Arthurs, A. Dalgarno, Proc. R. Soc. A **256**, 540 (1960)
30. J.T. Hougen, NBS Monograph **115** (US Gov. Print. Office, Washington, DC, 1970)
31. C.E. Moore, *Atomic energy levels* (US Dep. of Commerce, National Bureau of Standards, Washington, DC, 1971), Vol. 3
32. E. Czuchaj, H. Stoll, Chem. Phys. **248**, 1 (1999)
33. E. Czuchaj, H. Stoll, H. Preuss, J. Phys. B: At. Mol. Phys. **20**, 1477 (1987)
34. E. Czuchaj, J. Sienkiewicz, J. Phys. B **17**, 2251 (1984)
35. B.R. Johnson, J. Comput. Phys. **13**, 445 (1973)
36. K.J. Dietz, P. Dabkiewicz, H.J. Kluge, T. Kühl, H.A. Schuessler, J. Phys. B: At. Mol. Phys. **13**, 2749 (1988)
37. W.H. Breckenridge, O.K. Malmin, J. Chem. Phys. **76**, 1812 (1982)
38. M. Czajkowski, E. Walentynowicz, L. Krause, J. Quant. Spectr. Rad. Transf. **28**, 13 (1982); N.P. Penkin, T.P. Redko, Opt. Spectry. **57**, 598 (1984); H. Umemoto, T. Ohnuma, A. Masaki, Chem. Phys. Lett. **171**, 357 (1990)